Article

A subwavelength atomic array switched by a single Rydberg atom

Kritsana Srakaew [1,2], Pascal Weckesser [1,2], Simon Hollerith[1,2], David Wei [1,2], Daniel Adler [1,2,3], Immanuel Bloch [1,2,3] & Johannes Zeiher [1,2] ✉

Enhancing light–matter coupling at the level of single quanta is essential for numerous applications in quantum science. The cooperative optical response of subwavelength atomic arrays has been found to open new pathways for such strong light–matter couplings, while simultaneously offering access to multiple spatial modes of the light field. Efficient single-mode free-space coupling to such arrays has been reported, but spatial control over the modes of outgoing light fields has remained elusive. Here, we demonstrate such spatial control over the optical response of an atomically thin mirror formed by a subwavelength array of atoms in free space using a single controlled ancilla atom excited to a Rydberg state. The switching behaviour is controlled by the admixture of a small Rydberg fraction to the atomic mirror, and consequently strong dipolar Rydberg interactions with the ancilla. Driving Rabi oscillations on the ancilla atom, we demonstrate coherent control of the transmission and reflection of the array. These results represent a step towards the realization of quantum coherent metasurfaces, the demonstration of controlled atom–photon entanglement and deterministic engineering of quantum states of light.

Realizing efficient light–matter interfaces and engineering states of light at the quantum level are challenging due to the small interaction cross section between atoms and photons[1]. Overcoming this challenge requires enhanced coupling between light and matter, for example, via optical cavities[2–6] or waveguides[7–10] for single atoms, or by exploiting systems with high optical densities coupled to Rydberg states[11–14]. In optical cavities, for example, the presence or absence of a strongly coupled atom can be exploited to change the optical response of the cavity from transmitting to reflecting for impinging photons, the basis of photon–photon gates[15–17]. There, the enhanced interaction cross section, however, comes at the cost of a strong mode selection: optical cavities typically support only a single spatial mode for the photons, which limits their use for spatial light shaping. Ordered subwavelength arrays of emitters have recently emerged as an alternative approach to realizing strong light–matter coupling[18–26], with distinct advantages over disordered ensembles in applications such as photon storage[27] or photonic gates[28,29]. In these systems, emitters are periodically arranged at distances below the wavelength of light, resulting in

highly cooperative optical properties as a result of dipolar interactions. The free-space nature of cooperative arrays strongly relaxes the mode selection, which enables spatial control over the modes of single photons interacting with the array. In particular, such control was recently proposed by using strong interactions between highly excited atomic Rydberg states[28–30]. The properties of a cooperative array can thereby be altered through the excitation of a single atom to a Rydberg state, realizing a 'quantum-controlled metamaterial' as introduced by Bekenstein et al.[28], in which the optical response of the system can be changed in a spatially controlled way. Such control provides a fundamentally new approach to photonic state engineering in free space, with the perspective of creating large-scale photonic entangled states relevant for photonic quantum information applications[28]. Closely related proposals exploit a single atom to control the spatial photon mode via a dipole–dipole exchange interaction in an atomic ensemble[31] or a bilayer atomic array[32]. In contrast to schemes based on dissipation[11–13,33–35], where decay occurs randomly from the input channel into a large number of modes by free-space scattering,

[1]Max-Planck-Institut für Quantenoptik, Garching, Germany. [2]Munich Center for Quantum Science and Technology (MCQST), Munich, Germany. [3]Fakultät für Physik, Ludwig-Maximilians-Universität, Munich, Germany. ✉e-mail: johannes.zeiher@mpq.mpg.de
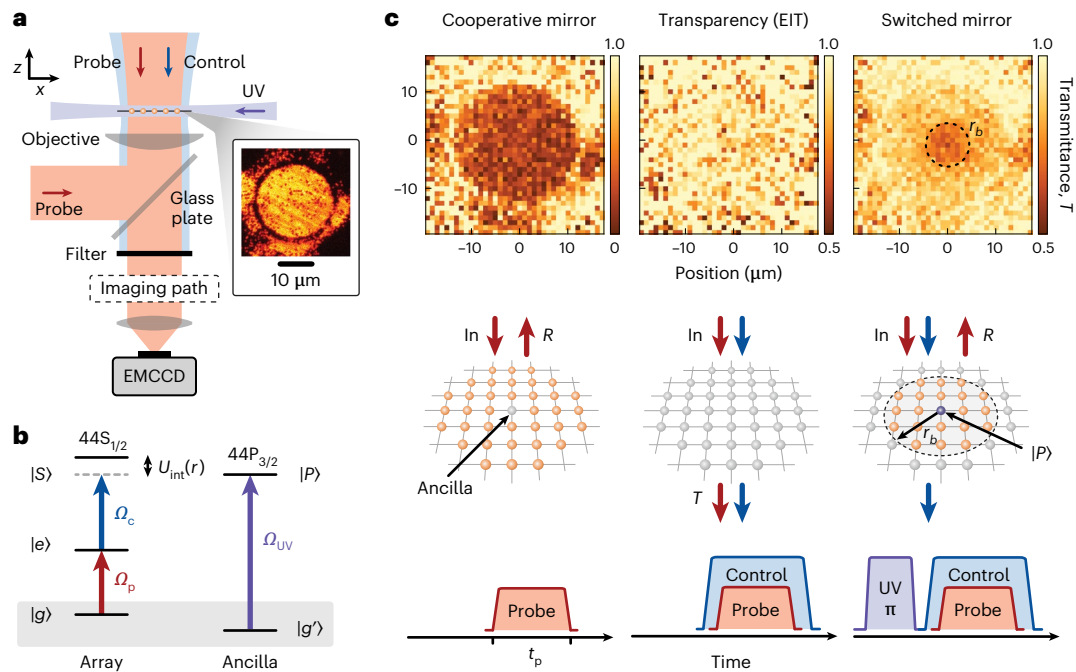
Fig. 1 | Schematic of the experiment. a, The atomic array and laser beam orientations. The transmission (reflection) probe beam is overlapped and co- (counter-)propagating with the control beam along −z (+z). We monitor the transmissive (reflective) response of the atomic array by imaging the probe beam onto an EMCCD, while filtering out the control beam. The atomic array is aligned in the x−y plane, containing up to 1,500 atoms in an atomic Mott insulator of a single atom per lattice site in state $|g\rangle$, while a single ancilla atom is prepared in a different hyperfine state $|g'\rangle$ at a target lattice site at the centre of the array. We control the Rydberg excitation of the ancilla using an ultraviolet (UV) beam propagating in the atomic plane. The inset shows an exemplary site-resolved fluorescence image of a Mott insulator with 1,500 atoms. **b**, Electronic level scheme and relevant light fields. The control and probe fields with Rabi frequencies Ω_c and Ω_p, respectively, couple the ground state $|g\rangle$ to a Rydberg

S-state $|S\rangle$ via an intermediate state $|e\rangle$. The UV field excites the ancilla $|g'\rangle$ with Rabi frequency Ω_{UV} to a Rydberg P-state of the same principal quantum number $|P\rangle$. The $|S\rangle - |P\rangle$ Rydberg states experience a strong dipolar interaction, creating a distance-dependent shift in energy, $U_{int}(r)$. **c**, Spatially resolved optical response in transmission, the atomic array with the relevant light fields and the corresponding experimental pulse sequences. Left: With the probe field alone, the atomic array acts as a cooperative mirror. Middle: Applying an additional resonant control field, we render the atomic array transparent by exploiting the EIT condition. Right: Preparing the ancilla in the $|P\rangle$ state, the dipolar Rydberg interaction shifts the control field out of resonance, restoring the reflectivity within a finite radius around the ancilla. The dashed line indicates the estimated blockade radius of $r_b = 4.6$ μm (Supplementary Information).

the cooperative array allows for coherent switching between various spatial light modes, such as the transmission and reflection of an atomic array. Furthermore, the cooperative optical response of ordered arrays dramatically reduces the atom number and density required to reach optical depths comparable to disordered ensembles[27,29]. Similar to recent work performed in optical cavities[17,36], they can therefore help to mitigate known systematics that limit the performance of disordered ensembles in free space at large atomic densities[33,37].

Here, we exploit the strong cooperative response of an array of ordered emitters separated by subwavelength distances to realize a switch for photons. This setup allows for recreating the prototypical situation encountered in strongly coupled cavity quantum electrodynamics, where single-atom control can be exploited to reroute single photons[6]. We utilize the strong interactions between Rydberg states of opposite parity to switch the optical properties of the array from transmitting to reflecting. We achieve spatial control by using an ancilla atom prepared with single-site precision at a specific target position within the array. We demonstrate that the optical properties of the array can be altered coherently by driving Rabi oscillations on the ancilla into the Rydberg state. Finally, we directly measure the spatial switching area of the ancilla in our system and present evidence that the residual imperfections in switching are dominated by the finite Rydberg lifetime and preparation fidelity of the ancilla, both straightforward to overcome with future upgrades to the experimental setup.

Analogous to recent experiments focused on quantum optics with Rydberg atoms[11,13,33], the key idea for controlling our subwavelength

array is to transfer the strong interactions between Rydberg states to the optical response of the cooperative array through electromagnetically induced transparency (EIT)[38]. We start with a cooperative atomic array with emitters approximately described as two-level systems with ground state $|g\rangle$ and excited state $|e\rangle$. To induce EIT, the excited state $|e\rangle$ is coupled with a control field Ω_c to a highly excited Rydberg S-state $|S\rangle$ (Fig. 1b). As a result, the cooperative optical two-level response for a weak probe field of Rabi frequency Ω_p, impinging normal on the array, is altered and the system becomes transparent on the $|g\rangle \leftrightarrow |e\rangle$ resonance in the presence of the control beam (Fig. 1c, middle column). In establishing transparency, the excited state $|S\rangle$ is admixed to the state $|e\rangle$ through the control field Ω_c. Consequently, $|e\rangle$ inherits some of the long-range interacting character of $|S\rangle$. The parameters Ω_c and Ω_p are chosen to keep the Rydberg state population sufficiently small to avoid optical nonlinearities due to self-blockade, which is expected when the probability to find any array atom in $|S\rangle$ approaches unity[11,39]. To control the properties of the cooperative mirror, an additional 'ancilla' atom in the ground state $|g'\rangle$ is excited to a neighbouring Rydberg P-state $|P\rangle$.

Due to strong Rydberg interactions between $|S\rangle$ and $|P\rangle$, the state $|S\rangle$ is shifted in energy by $U_{int}(r)$. This interaction shift exceeds half of the EIT spectral width within a 'blockade disc' of radius r_b (refs. [40,41]) centred around the location of the ancilla. Consequently, the EIT condition breaks down and the optical properties return to those of the cooperative mirror. Due to its coherent nature, the single ancilla atom can entangle the mirror response with the ancilla state, which can
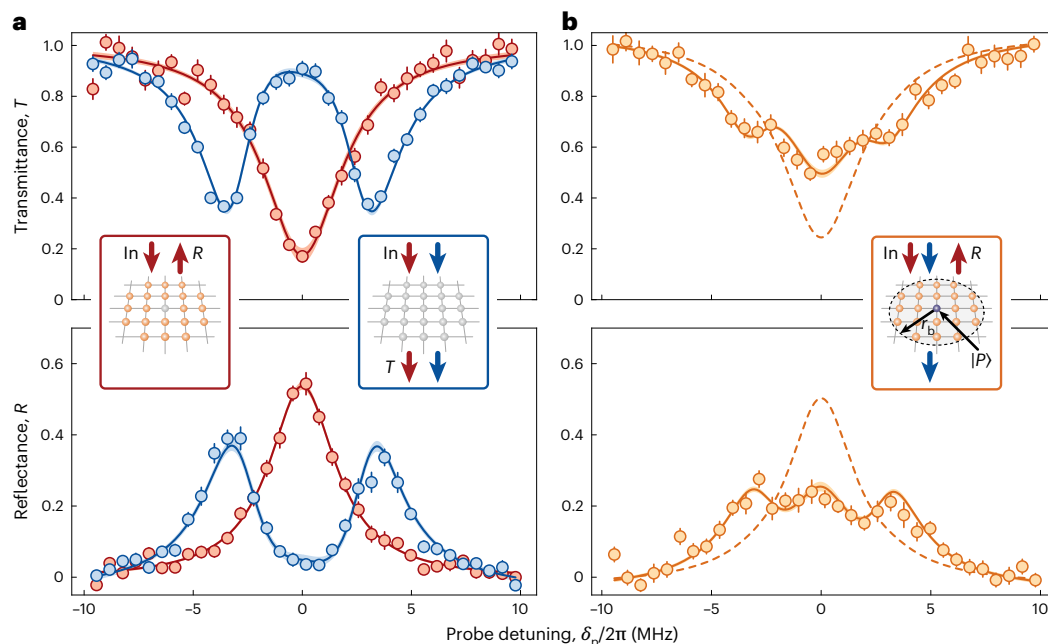
Fig. 2 | Cooperative response in the absence and presence of the Rydberg ancilla. a, The cooperative response of the atomic array with (blue) and without (red) the control beam for a probe duration of $t_p = 20$ μs and the ancilla prepared in $|g'\rangle$. Without the control laser, we reproduce the cooperative subradiant response of the mirror with a transmission and reflection linewidth $\Gamma_M/2\pi$ of 4.40(32) or 3.75(14) MHz, respectively. With the control laser present, we observe a splitting of the single peak into an EIT doublet, where the width of each peak $\Gamma_{EIT}/2\pi$ amounts to 2.95(17) and 3.01(28) MHz in transmission and reflection, respectively, and a minimal transmittance and maximal reflectance of 0.35(2) and 0.37(2), respectively, is observed. **b**, Preparing the ancilla atom in the Rydberg state $|P\rangle$, the spectra change dramatically, and reveal a triple-peak structure, featuring contributions of both the cooperative mirror and EIT spectrum.

Superimposing both spectra while having the ancilla Rydberg fraction $P_{|P\rangle}$ and a global offset as free fit parameters (solid orange lines), we find excellent agreement with our data set with $P_{|P\rangle}$ of 0.61(2) and 0.45(2) in transmittance and reflectance, respectively, in good agreement with an independent reference measurement of $P_{|P\rangle} = 0.52(8)$ (Supplementary Information). The dashed orange lines illustrate the expected spectra assuming ideal ancilla preparation and substantially shorter probe duration than the Rydberg lifetime ($t_p = 2$ μs), improving the ancilla Rydberg fraction to $P_{|P\rangle} = 0.96$. The insets in each figure illustrate the atomic array and beam directions for each experimental configuration. The red (blue) arrows indicate the incident and scattered probe (control) beam directions. The measurements are averages over 70–125 independent repetitions. Error bars denote the s.e.m.

subsequently be exploited for photonic state engineering[28]. Furthermore, controlling the position of the ancilla atom within the array enables full spatial control over the optical properties of the array (Fig. 1c). In particular, using this scheme, optical modes with diameters of a few lattice sites can be controlled without compromising the cooperativity of the response[27].

We began our experiments by preparing a nearly unity filled two-dimensional atomic array of ^{87}Rb atoms spin-polarized in the state $|g\rangle = |5S_{1/2}, F = 2, m_F = -2\rangle$ in a single vertical antinode of a three-dimensional optical lattice with lattice constant $a_{lat} = 532$ nm. The lattice spacing was below the transition wavelength $\lambda_p = 780$ nm from the ground state $|g\rangle$ to the excited state $|e\rangle = |5P_{3/2}, F = 3, m_F = -3\rangle$ leading to a cooperative response of the array at a ratio of $a_{lat}/\lambda_p = 0.68$ (ref. [25]). To enable control of the optical response of the mirror via Rydberg interactions, we coupled the excited state $|e\rangle$ to the $|S\rangle = |44S_{1/2}, m_J = -1/2\rangle$ Rydberg state. The optical properties of the array were probed with a weak probe beam with Rabi coupling $\Omega_p/2\pi = 168(5)$ kHz $\ll \Omega_c/2\pi = 6.7(6)$ MHz on the $|g\rangle \leftrightarrow |e\rangle$ transition, which is sufficient to create the EIT window and admix a small Rydberg amplitude to the excited state $|e\rangle$ (ref. [38]). We deterministically created a single ancilla atom in the $|g'\rangle = |5S_{1/2}, F = 1, m_F = -1\rangle$ state with a fidelity of 0.83(4) at the centre of the array using single-site addressing[42,43]. The ancilla was then controllably excited to the Rydberg state $|P\rangle = |44P_{3/2}, m_J = 3/2\rangle$ on an ultraviolet (UV) transition at a wavelength of 297 nm. The interaction with the admixed $|S\rangle$ state Rydberg fraction of the array atoms led to a Förster-enhanced energy shift $U_{int}(r)$, featuring a characteristic van der Waals distance dependence proportional to C_6/r^6 due to interactions with nearby Zeeman sublevels

(Supplementary Information). For our parameters, this resulted in a blockade radius $r_b = (2C_6\Gamma_e/\Omega_c^2)^{1/6} = 4.6$ μm (Supplementary Information) which defined the range over which the mirror properties are altered. Preparing an atomic array with a radius $r_a \gg r_b$ and detecting the probe light with a low-noise electron-multiplying change-coupled device (EMCCD) camera, we directly reveal the spatially switched area and demonstrate the spatially selective response of our array (Fig. 1c). To suppress the effect of long-range dipolar exchange of the ancilla[41,44], we work in a regime $r_a \approx r_b$ for the following characterization of the switching response of the array (Supplementary Information).

In a first set of experiments, we aim to demonstrate the basic mechanism of switching the cooperative mirror by using the ancilla atom. To this end, we first confirm the cooperative nature of our atomic array by measuring the reflection and transmission response of a laser beam tuned near the resonance of the $|g\rangle \leftrightarrow |e\rangle$ transition. We find a strong directional signal with a subradiant Lorentzian lineshape and an extracted width of down to $\Gamma_M/2\pi = 3.75(14)$ MHz, narrower than the natural linewidth of $\Gamma_e/2\pi = 6.06$ MHz (Fig. 2a). This confirms that our array is in the cooperative regime explored previously[25]. Illuminating the array with both the probe and control fields on resonance, we observe EIT, resulting in a switching from a reflecting to transmitting atom array. Scanning the probe detuning, we observe that the dip in transmission (peak in reflection) splits into a doublet with splitting Ω_c, demonstrating the effects of the control field. Interestingly, this doublet again shows signatures of a cooperative response, with a high level of reflectance of 0.37(2), exceeding the reflectance signal for isotropic scattering 0.16(3) (Supplementary Information). The width of each peak amounts to $\Gamma_{EIT}/2\pi = 2.95(17)$ MHz, consistent with the width in

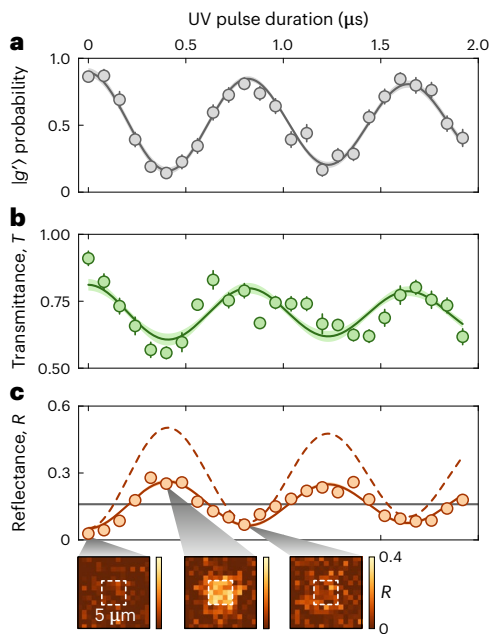**a**, Ancilla $|g'\rangle \leftrightarrow |P\rangle$ Rabi oscillations obtained from ground state $|g'\rangle$ fluorescence detection by varying the length of the UV pulse before probing (see Fig. 1c for the protocol). Applying a damped sinusoidal fit, we find a Rabi frequency of $\Omega_{UV}/2\pi = 1.22(2)$ MHz and a decay constant of $\tau_{decay} = 6(3)$ µs. **b,c**, The transmittance (**b**) and reflectance (**c**) data follow the Rabi oscillation of the ancilla. The solid lines in **b** and **c** represent the best fit results, with the amplitude of the oscillation and overall offset as the only fit parameters, while the oscillation frequency and decay time are fixed and taken from **a**. The three insets in **c** indicate spatially averaged reflection images for $\Omega_{UV}t = 0$, π and 2π, respectively, with an indicated region of interest of 5 µm × 5 µm. The dashed line in **c** illustrates the expected transmission signal for an ancilla Rydberg fraction of $P_{|P\rangle} = 0.96$. The solid grey line represents the resonance reflection signal (0.16(3)) from isotropic scattering. The latter was measured experimentally by introducing vertical disorder by means of Bloch oscillations (Supplementary Information). The measurements are averages over 120–170 independent repetitions. Error bars denote the s.e.m.

Fig. 4 | Distribution of detected photon number and lifetime. The detected photon number distribution, relative to the mean background photon number, in reflection within a region of interest, by preparing the ancilla in either the $|g'\rangle$ (blue) or the $|P\rangle$ (orange) state. For the former, we obtain a Poissonian distribution ($N = 1000$ repetitions) corresponding to the photon counts in the EIT configuration (solid blue line). Preparing the ancilla in $|P\rangle$, the histogram acquires a tail towards high reflected photon numbers ($N = 1300$ repetitions). This histogram is a combination of counts due to Rydberg-induced reflection (dashed orange line), and counts at low photon numbers due to imperfect Rydberg preparation and Rydberg decay. A Monte Carlo simulation including our experimental uncertainties reproduces the essential features of the observed histogram (solid orange line and shaded region; see Supplementary Information). The inset displays the transmission signal (T) for variable delay time δt between Rydberg excitation and probe pulse (70 repetitions). We extract the Rydberg lifetime of $\tau = 27(5)$ µs from an exponential fit (solid line). The dashed green line is the expected transmission signal for an ancilla Rydberg fraction of $P_{|P\rangle} = 0.96$. Error bars denote the s.e.m.

the single-particle limit of $\Gamma_e/2$. Our parameters were chosen to maximize the on-resonance contrast between the cooperative mirror and the EIT response using a probe duration $t_p = 20$ µs, only slightly shorter than the measured lifetime $\tau = 27(5)$ µs of the Rydberg ancilla. The probe power and pulse duration were chosen to keep the Rydberg admixture and the effects of self-blockade small, while providing sufficient signal-to-noise ratio of the probe light on the EMCCD camera (Supplementary Information).

To investigate the effect of the Rydberg ancilla on the array, we apply a π pulse on the $|g'\rangle \leftrightarrow |P\rangle$ transition with duration t, such that $\Omega_{UV}t = \pi$. The resulting spectra exhibit a broad resonance featuring a substructure of three distinct peaks, with the reflectance on resonance amounting to 0.25(2) (Fig. 2b). Our observation of a triple-peak structure can be understood to arise from a combination of the configurations with and without the ancilla Rydberg atom present. A simplified model assuming a statistical mixture of the mirror in the switched and unswitched state, weighted with the probability of finding the ancilla in the Rydberg or ground state, respectively, quantitatively reproduces the observed features in Fig. 2b. The ansatz of a statistical mixture of the two mirror states is motivated by imperfect initial state preparation of the ancilla in $|g'\rangle$ and decay of the ancilla Rydberg state during probing (Supplementary Information). To illustrate potential improvements in an upgraded experimental setup, the dashed lines in Fig. 2b also show the expected spectra for perfect ancilla preparation in $|g'\rangle$ and
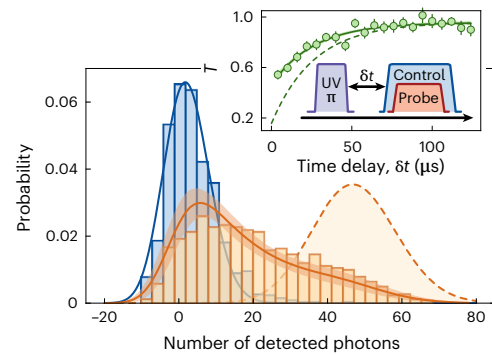
substantially shorter probe duration of $t_p = 2$ µs, for which on the order of one photon is scattered, and the decay of the Rydberg ancilla becomes negligible.

To highlight the capability of coherent manipulation in our system, we next aim to dynamically change the optical properties of the atomic array. To this end, we drive the ancilla from the ground state $|g'\rangle$ to the Rydberg state $|P\rangle$ with variable UV pulse durations, resulting in coherent Rabi oscillations of the ancilla with a Rabi frequency of $\Omega_{UV}/2\pi = 1.22(2)$ MHz (Fig. 3). Measuring the transmittance or reflectance of the array in the same sequence, we find a strong correlation between ancilla Rabi oscillations and the optical properties of the array, where the mirror switches from transmitting to reflecting during the course of the oscillations. Fitting the dynamics of transmittance and reflectance of the array with a damped sinusoidal function derived from the Rabi oscillations with the amplitude and offset of the oscillation as free parameters, we find excellent agreement between this model and the data. This agreement indicates that, indeed, the switching behaviour is determined by the quantum state of the ancilla before probing. The small distortions in the transmittance can be attributed to a non-vanishing probability to initially have two ancilla atoms before excitation to the Rydberg state (Supplementary Information). Notably, the maxima of the oscillating reflectance are clearly above the single-particle limit of a vertically disordered array (ref. [25] and Supplementary Information) demonstrating that the cooperative response of the mirror is preserved during the oscillation (Fig. 3c).

The strong correlation between the state of the ancilla and the state of the mirror can be further studied through photon number statistics. In the ideal case, we expect all photons within a detection window to be reflected (transmitted) when the ancilla is excited to the Rydberg state $|P\rangle$ (in its ground state $|g'\rangle$). We study this correlation by monitoring the number of reflected photons for a longer integration time of $t_p = 60$ µs after controllably exciting the ancilla with a π pulse (Fig. 4). The distribution with the ancilla in $|P\rangle$ exhibits a long tail at high
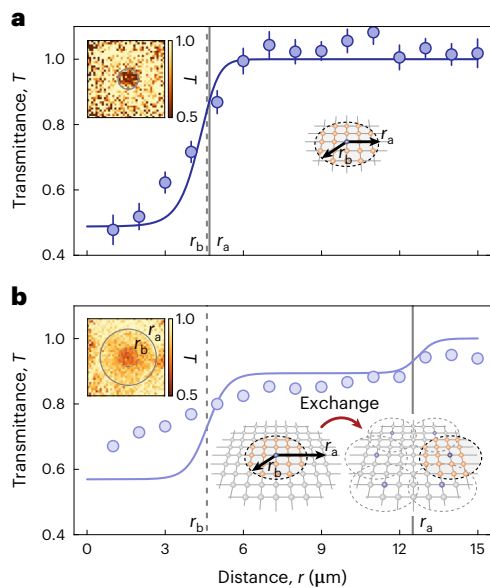
Fig. 5 | Spatially resolved switching area. The radially averaged transmittance over the size of the switched mirror, centred around the ancilla atom. The solid lines show the estimated radial profile, including $|S\rangle - |P\rangle$ blockade, array size and Rydberg fraction of the ancilla $P_{|P\rangle}$. **a**, The transmittance of the array containing 250 atoms, comparable in size ($r_a \approx 4.7$ µm) to the blockade radius, shows good agreement with the estimated radial profile (120 repetitions). **b**, The array of 1,500 atoms with radius $r_a \approx 12.5$ µm, large compared with the blockade radius, shows a washing out of the transmittance versus distance, deviating from the solid line (3,500 repetitions). This can be explained by long-range exchange processes, where the $|P\rangle$ excitation undergoes $|S\rangle - |P\rangle$ exchange resulting in the transport of the excitation and therefore a shift of the switching area as illustrated by the sketch. The insets on the upper left for both **a** and **b** illustrate the spatially averaged transmission images of the small and large array, respectively. The vertical solid and dashed lines mark the array radius r_a (estimated blockade radius r_b). The radii are further indicated in the upper left insets of the averaged transmission images. Error bars denote the s.e.m.

numbers of reflected photons in addition to a peak at low photon numbers. We find good agreement of our observed histogram with a model taking into account our estimated preparation fidelity as well as the independently measured lifetime of the Rydberg-excited ancilla via Monte Carlo sampling (Supplementary Information and Fig. 4).

The spatial control over the position of the ancilla allows for a fundamentally new approach to controlling the optical response of the subwavelength array in a spatially resolved way. To demonstrate such control, we prepared the ancilla at a target site in the centre of the array and compared the optical response of a small array of radius $r_a = 4.7(7)$ µm with a larger array with radius of $r_a = 12.5(5)$ µm, which exceeds the expected blockade radius (Fig. 5). In the small array, we observe a relatively sharp edge where the transmission jumps from its central value of 0.48(2) to near unity, due to the combination of the finite size of the array r_a and the blockade radius r_b. In contrast, the large array has an increased transmittance at the centre as well as a more gradual increase of the transmittance beyond the blockade radius. These observations indicate the presence of previously studied long-range exchange processes[41,44], which cause the ancilla to delocalize over the entire system and lead to a smoothened transmission signal. Importantly, these exchange processes can be suppressed either by operating on shorter probe timescales or by reducing the probe power, as the relevant exchange process scales with $\propto \Omega_p^2$ (ref. [44] and Supplementary Information). This regime is experimentally accessible with optimized detectors matched to the manipulated spatial modes of the light field, which, however, would not have allowed for the

spatially resolved proof-of-principle characterization of the array response performed in this work.

In conclusion, we have demonstrated the ability to switch and coherently control the optical properties of a cooperative subwavelength array of atoms using a single ancilla atom. Our system is presently limited by finite preparation efficiencies as well as the finite Rydberg lifetime of the ancilla. The former can be improved by better addressing techniques, for example, by placing the ancilla in a single microtrap overlapped with the cooperative array, and the latter with optimized single-photon detectors. Alternatively, we foresee the use of Rydberg dressing[45] for the ancilla, improving its lifetime while minimizing motional decoherence effects due to reduced repulsion in the lattice and the suppression of dipolar exchange processes.

Our measurements already demonstrate all the experimental building blocks to control single photons by manipulating single atoms in subwavelength arrays and open the path towards the detection of atom–photon entanglement[46], the realization of photon–photon gates[28,47] or multimode quantum optics in cooperative arrays[28–30].

Online content

Any methods, additional references, Nature Portfolio reporting summaries, source data, extended data, supplementary information, acknowledgements, peer review information; details of author contributions and competing interests; and statements of data and code availability are available at https://doi.org/10.1038/s41567-023-01959-y.

References

1. Chang, D. E., Douglas, J. S., González-Tudela, A., Hung, C.-L. & Kimble, H. J. Colloquium: quantum matter built from nanoscopic lattices of atoms and photons. *Rev. Mod. Phys.* **90**, 031002 (2018).
2. Kimble, H. J. Strong interactions of single atoms and photons in cavity QED. *Phys. Scr.* **T76**, 127 (1998).
3. McKeever, J. et al. Deterministic generation of single photons from one atom trapped in a cavity. *Science* **303**, 1992–1994 (2004).
4. Birnbaum, K. M. et al. Photon blockade in an optical cavity with one trapped atom. *Nature* **436**, 87–90 (2005).
5. Mücke, M. et al. Electromagnetically induced transparency with single atoms in a cavity. *Nature* **465**, 755–758 (2010).
6. Reiserer, A. & Rempe, G. Cavity-based quantum networks with single atoms and optical photons. *Rev. Mod. Phys.* **87**, 1379–1418 (2015).
7. Junge, C., O'Shea, D., Volz, J. & Rauschenbeutel, A. Strong coupling between single atoms and nontransversal photons. *Phys. Rev. Lett.* **110**, 213604 (2013).
8. Thompson, J. D. et al. Coupling a single trapped atom to a nanoscale optical cavity. *Science* **340**, 1202–1205 (2013).
9. Lodahl, P., Mahmoodian, S. & Stobbe, S. Interfacing single photons and single quantum dots with photonic nanostructures. *Rev. Mod. Phys.* **87**, 347–400 (2015).
10. Lodahl, P. et al. Chiral quantum optics. *Nature* **541**, 473–480 (2016).
11. Peyronel, T. et al. Quantum nonlinear optics with single photons enabled by strongly interacting atoms. *Nature* **488**, 57–60 (2012).
12. Dudin, Y. O. & Kuzmich, A. Strongly interacting Rydberg excitations of a cold atomic gas. *Science* **336**, 887–889 (2012).
13. Firstenberg, O., Adams, C. S. & Hofferberth, S. Nonlinear quantum optics mediated by Rydberg interactions. *J. Phys. B* **49**, 152003 (2016).
14. Thompson, J. D. et al. Symmetry-protected collisions between strongly interacting photons. *Nature* **542**, 206–209 (2017).
15. Duan, L.-M. & Kimble, H. J. Scalable photonic quantum computation through cavity-assisted interactions. *Phys. Rev. Lett.* **92**, 127902 (2004).

16. Hacker, B., Welte, S., Rempe, G. & Ritter, S. A photon–photon quantum gate based on a single atom in an optical resonator. *Nature* **536**, 193–196 (2016).

17. Stolz, T. et al. Quantum-logic gate between two optical photons with an average efficiency above 40%. *Phys. Rev. X* **12**, 021035 (2022).

18. Porras, D. & Cirac, J. I. Collective generation of quantum states of light by entangled atoms. *Phys. Rev. A* **78**, 053816 (2008).

19. Jenkins, S. D. & Ruostekoski, J. Controlled manipulation of light by cooperative response of atoms in an optical lattice. *Phys. Rev. A* **86**, 031602 (2012).

20. Jenkins, S. D. & Ruostekoski, J. Metamaterial transparency induced by cooperative electromagnetic interactions. *Phys. Rev. Lett.* **111**, 147401 (2013).

21. Facchinetti, G., Jenkins, S. D. & Ruostekoski, J. Storing light with subradiant correlations in arrays of atoms. *Phys. Rev. Lett.* **117**, 243601 (2016).

22. Bettles, R. J., Gardiner, S. A. & Adams, C. S. Enhanced optical cross section via collective coupling of atomic dipoles in a 2D array. *Phys. Rev. Lett.* **116**, 103602 (2016).

23. Shahmoon, E., Wild, D. S., Lukin, M. D. & Yelin, S. F. Cooperative resonances in light scattering from two-dimensional atomic arrays. *Phys. Rev. Lett.* **118**, 113601 (2017).

24. Asenjo-Garcia, A., Moreno-Cardoner, M., Albrecht, A., Kimble, H. J. & Chang, D. E. Exponential improvement in photon storage fidelities using subradiance and "selective radiance" in atomic arrays. *Phys. Rev. X* **7**, 031024 (2017).

25. Rui, J. et al. A subradiant optical mirror formed by a single structured atomic layer. *Nature* **583**, 369–374 (2020).

26. Solntsev, A. S., Agarwal, G. S. & Kivshar, Y. S. Metasurfaces for quantum photonics. *Nat. Photonics* **15**, 327–336 (2021).

27. Manzoni, M. T. et al. Optimization of photon storage fidelity in ordered atomic arrays. *New J. Phys.* **20**, 083048 (2018).

28. Bekenstein, R. et al. Quantum metasurfaces with atom arrays. *Nat. Phys.* **16**, 676–681 (2020).

29. Moreno-Cardoner, M., Goncalves, D. & Chang, D. E. Quantum nonlinear optics based on two-dimensional Rydberg atom arrays. *Phys. Rev. Lett.* **127**, 263602 (2021).

30. Zhang, L., Walther, V., Mølmer, K. & Pohl, T. Photon-photon interactions in Rydberg-atom arrays. *Quantum* **6**, 674 (2022).

31. Petrosyan, D. & Mølmer, K. Deterministic free-space source of single photons using Rydberg atoms. *Phys. Rev. Lett.* **121**, 123605 (2018).

32. Grankin, A., Guimond, P. O., Vasilyev, D. V., Vermersch, B. & Zoller, P. Free-space photonic quantum link and chiral quantum optics. *Phys. Rev. A* **98**, 043825 (2018).

33. Baur, S., Tiarks, D., Rempe, G. & Dürr, S. Single-photon switch based on Rydberg blockade. *Phys. Rev. Lett.* **112**, 073901 (2014).

34. Gorniaczyk, H., Tresp, C., Schmidt, J., Fedder, H. & Hofferberth, S. Single-photon transistor mediated by interstate Rydberg interactions. *Phys. Rev. Lett.* **113**, 053601 (2014).

35. Xu, W. et al. Fast preparation and detection of a Rydberg qubit using atomic ensembles. *Phys. Rev. Lett.* **127**, 050501 (2021).

36. Vaneecloo, J., Garcia, S. & Ourjoumtsev, A. Intracavity Rydberg superatom for optical quantum engineering: coherent control, single-shot detection, and optical π phase shift. *Phys. Rev. X* **12**, 021034 (2022).

37. Tiarks, D., Schmidt-Eberle, S., Stolz, T., Rempe, G. & Dürr, S. A photon–photon quantum gate based on Rydberg interactions. *Nat. Phys.* **15**, 124–126 (2019).

38. Fleischhauer, M., Imamoglu, A. & Marangos, J. P. Electromagnetically induced transparency: optics in coherent media. *Rev. Mod. Phys.* **77**, 633–673 (2005).

39. Pritchard, J. D. et al. Cooperative atom–light interaction in a blockaded Rydberg ensemble. *Phys. Rev. Lett.* **105**, 193603 (2010).

40. Günter, G. et al. Interaction enhanced imaging of individual Rydberg atoms in dense gases. *Phys. Rev. Lett.* **108**, 013002 (2012).

41. Günter, G. et al. Observing the dynamics of dipole-mediated energy transport by interaction-enhanced imaging. *Science* **342**, 954–956 (2013).

42. Weitenberg, C. et al. Single-spin addressing in an atomic Mott insulator. *Nature* **471**, 319–324 (2011).

43. Fukuhara, T. et al. Quantum dynamics of a mobile spin impurity. *Nat. Phys.* **9**, 235–241 (2013).

44. Schempp, H., Günter, G., Wüster, S., Weidemüller, M. & Whitlock, S. Correlated exciton transport in Rydberg-dressed-atom spin chains. *Phys. Rev. Lett.* **115**, 093002 (2015).

45. Jau, Y.-Y., Hankin, A. M., Keating, T., Deutsch, I. H. & Biedermann, G. W. Entangling atomic spins with a Rydberg-dressed spin-flip blockade. *Nat. Phys.* **12**, 71–74 (2016).

46. Li, L., Dudin, Y. O. & Kuzmich, A. Entanglement between light and an optical atomic excitation. *Nature* **498**, 466–469 (2013).

47. Gorshkov, A. V., Otterbach, J., Fleischhauer, M., Pohl, T. & Lukin, M. D. Photon-photon interactions via Rydberg blockade. *Phys. Rev. Lett.* **107**, 133602 (2011).

Author contributions

K.S. acquired the data and, together with P.W., D.W. and D.A., maintained and improved the experimental setup. P.W. and S.H. contributed the theoretical simulations. I.B. and J.Z. supervised the study. All authors worked on the interpretation of the data and contributed to the final manuscript.

Additional information

Supplementary information The online version contains supplementary material available at https://doi.org/10.1038/s41567-023-01959-y.

Correspondence and requests for materials should be addressed to Johannes Zeiher.

Peer review information *Nature Physics* thanks the anonymous reviewers for their contribution to the peer review of this work.

Reprints and permissions information is available at www.nature.com/reprints.